Journal of Neuro-Oncology **53:** 161–176, 2001.

Glioma cell motility is associated with reduced transcription of proapoptotic and proliferation genes: a cDNA microarray analysis

Luigi Mariani[1], Christian Beaudry[1], Wendy S. McDonough[1], Dominique B. Hoelzinger[1], Tim Demuth[1], Kristen R. Ross[1], Theresa Berens[1], Stephen W. Coons[1], George Watts[2], Jeffrey M. Trent[3], Jun S. Wei[3], Alf Giese[4] and Michael E. Berens[1]
[1]*Neuro-Oncology Laboratory, Barrow Neurological Institute, Phoenix, AZ;* [2]*Arizona Cancer Center, Microarray Core Facility, Tucson, AZ;* [3]*National Human Genome Research Institute, National Institutes of Health, Bethesda, MD, USA;* [4]*Neurochirurgische Klinik, UKE, Hamburg, Germany*

Key words: apoptosis, cDNA microarray, glioma, migration, proliferation

Summary

Microarray analysis of complementary DNA (cDNA) allows large-scale, comparative, gene expression profiling of two different cell populations. This approach has the potential for elucidating the primary transcription events and genetic cascades responsible for increased glioma cell motility *in vitro* and invasion *in vivo*. These genetic determinants could become therapeutic targets.

We compared cDNA populations of a glioma cell line (G112) exposed or not to a motility-inducing substrate of cell-derived extracellular matrix (ECM) proteins using two sets of cDNA microarrays of 5700 and 7000 gene sequences. The data were analyzed considering the level and consistency of differential expression (outliers) and whether genes involved in pathways of motility, apoptosis, and proliferation were differentially expressed when the motility behavior was engaged. Validation of differential expression of selected genes was performed on additional cell lines and human glioblastoma tissue using quantitative RT-PCR.

Some genes involved in cell motility, like tenascin C, neuropilin 2, GAP43, PARG1 (an inhibitor of Rho), PLCγ, and CD44, were over expressed; other genes, like adducin 3γ and integrins, were down regulated in migrating cells. Many key cell cycle components, like cyclin A and B, and proliferation markers, like PCNA, were strongly down regulated on ECM. Interestingly, genes involved in apoptotic cascades, like Bcl-2 and effector caspases, were differentially expressed, suggesting the global down regulation of proapoptotic components in cells exposed to cell-derived ECM. Overall, our findings indicate a reduced proliferative and apoptotic activity of migrating cells. cDNA microarray analysis has the potential for uncovering genes linking the phenotypic aspects of motility, proliferation, and apoptosis.

Introduction

The malignant phenotype is characterized by clonal cell expansion, immortalization, loss of contact inhibition, and the ability to invade locally as well as at a distance (metastasis). In the context of astrocytomas, local invasion, and not metastasis, is one of the main confounding factors to effective treatment. The ability to diffusely invade the normal brain is the hallmark of astrocytomas and this tendency increases with histological grade. Local invasion requires changes in cell–cell interactions, cell–extracellular matrix (ECM) interactions, and intracellular changes resulting in increased and directional motility into the normal brain. Controlling the invasive phenotype would result in reducing further spread of malignant cells. Because of the potential interdependence of apoptotic, proliferative, and motility-related pathways, a profound effect can be expected on the tumor cells once their invasiveness has been controlled.

The invasive phenotype is difficult to elucidate *in vivo*. However, there is a good correlation between increased invasiveness *in vivo* and increased motility *in vitro* [1,2]. Motility of glioblastoma cells can be

readily stimulated *in vitro*, mainly through the use of extracellular matrix proteins [2–6].

Microarrays of cDNA sequences are a powerful tool to explore on a large scale the gene expression profile of a cell population with a particular phenotype [1,7,8], in the present instance the motility phenotype. In this study, we compared on two different microarrays the relative levels of expression of about 5000 and 7000 gene sequences by a glioma cell line when it was exposed to the ECM (motility-activating) produced by another glioma cell line, SF767 [9,10]. This substrate was selected among other cell-derived matrices because it has the advantage of strongly stimulating motility of most of the cell lines tested [11]. Also, because it is produced by glioma cells, it is likely to at least partially reflect the *in vivo* invasion matrix [12]. The composition of this matrix is largely undefined, although it contains tenascin C by Western blot analysis (unpublished). As a reference substrate, the same cell line was propagated on plain culture flasks in the presence of serum. This is not a condition of arrested migration, since ECM proteins like vitronectin and fibronectin are present in the serum and may serve as factors utilized for cell attachment and spreading [13,14]. However, in relative terms, cell-derived ECM induced a strong migratory response of G112 cells (Figure 1).

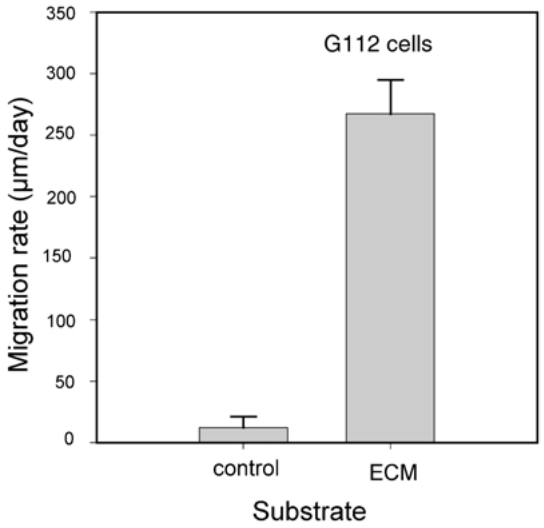

Figure 1. Accelerated migration rate on cell-derived ECM. The assay showed that the migration rate of G112 glioma cells was strongly accelerated when the cells were seeded on cell-derived ECM compared to the controls on a nonspecific protein substrate, bovine serum albumin.

We analyzed genes that were strongly differentially expressed regardless of their identity (statistical outliers). We then specifically analyzed the relative expression level of genes known to play a role in cell motility, proliferation, and apoptosis.

Methods

Cell lines and tissue

Human glioma cell lines G112 [15], SF767 [9,10], and T-98g [16] were serially propagated in minimum essential media supplemented with 10% fetal calf serum. Three human biopsy specimens of brain tumor were surgically removed under IRB-approved protocol, then immediately cryopreserved in liquid nitrogen. Confirmed diagnosis of glioblastoma multiforme (WHO) was made in paraffin-embedded tissue by S.W. Coons.

Production of cell-derived ECM

To create a coating of cell-derived ECM proteins, culture flasks (Corning) were seeded with SF767 glioma cells. The cells were grown to post-confluence, removed by treatment with Triton X-100 0.5% for 30 min at room temparature (RT), followed by NH_4OH 0.25 M 3–5 min at RT, then thoroughly rinsed with phosphate-buffered saline (PBS) [17,18]. This treatment disrupts cell membranes and removes cellular debris leaving in place the assembled substances and factors secreted by SF767 cells, called cell-derived ECM. The flasks covered with cell-derived ECM were stored at 4°C until used. G112 glioma cells were seeded either on uncoated tissue culture flasks (control) or on ECM-coated flasks to induce a migratory phenotype. The cells were grown for 2–3 days until they reached 40–60% confluence, then they were trypsinized, counted, and further processed for RNA isolation and synthesis of cDNA.

Migration assay

The microliter scale migration assay has been detailed previously [4] and has recently been used to verify *in vitro* the invasive phenotype observed *in vivo* [1]. Briefly, 10-well teflon-masked microscope slides were left untreated or coated with laminin 10 µg/ml at 37°C for 1 h, then blocked with BSA 1%. Approximately 2500 cells/well were seeded through a cell

sedimentation manifold (CSM Inc., Phoenix, AZ) to establish a circular confluent monolayer within 1 mm diameter at the center of the substrate-coated well. Cells were allowed to migrate during 24 h in MEM supplemented with 10% FBS at 37°C. The migration rate was calculated as the radius increase of the entire cell population. Experiments were performed as five replicates.

Isolation of RNA, synthesis of fluorescence cDNA, and hybridization on microarray slides

Approximately 40 million cells/sample were harvested by trypsinization for isolation of total RNA (Qiagen RNeasy® Maxi Kit). Total RNA was further purified with TRIzol (Life Technologies®); RNA concentrations were measured by spectrophotometry and normalized accordingly. For analysis on the 5 K microarray slide at the Arizona Cancer Center (AZCC), messenger RNA (mRNA) was further purified from total RNA using the Oligotex™ mRNA Midi-Kit (Qiagen®). Samples for both microarrays were reverse transcribed using SuperScript II reverse transcriptase (Life Technologies®), incorporating Cy3-dUTP in cDNA from 80 μg total RNA (or 1–3 μg mRNA) from cells grown on plastic and Cy5-dUTP in cDNA from 150 μg total RNA (or 1–3 μg mRNA) from cells grown on ECM. In a separate reverse transcription reaction for an independent hybridization, each cDNA was labeled with the reciprocal fluorochrome. This reciprocal labeling, yielding a second set of data, was performed exclusively on the 7 K microarray slide of the National Institute of Health (NIH). cDNA probes were purified and concentrated with Microcon-30 columns (Amicon®) mixed with a hybridization cocktail containing 15 μg poly dA, 6 μg yeast tRNA, 15 μg CoT 10 DNA, 2 × Denhards, 2.7 × SSC and 0.2% SDS, denatured and hybridized for 16 h at 65°C on a 5 K cDNA microarray (AZCC) or a 6.712 K cDNA microarray slide (NIH). Slides were washed in 0.1% sodium dodecylsulfate (SDS) with 0.5 × SSC, 0.01% SDS with 0.5 × SSC and 0.06 × SSC for 2 min each at room temperature, then scanned for analysis of fluorescence emission from each spot at 570 and 670 nm for Cy3 and Cy5, respectively [1,19–21].

Normalization of levels of fluorescence and analysis of the relative expression levels

Two cDNA populations, one labeled with the fluorochrome Cy3 and the other with the fluorochrome Cy5, were incubated to allow hybridization with the complementary gene sequences printed on the array. After normalization of the difference in fluorescence signal intensity of each dye on a cassette of housekeeping genes on the chips, the relative fluorescence intensity of each of the fluorochromes on each microarrayed spot portrayed the relative abundance of the hybridizing cDNAs from the two samples.

AZCC microarray. A median intensity of a spot of 1.4× above background intensity in both channels was the minimum requirement to qualify for calculation of expression ratios. Background intensity was assessed by measuring non-specific hybridization to cDNA sequences lacking homology to human genes (ice plant genes). The raw levels of fluorescence recorded from each microarray spot were subsequently corrected and analyzed as follows: (1) Normalize the intensity values in the two fluorescent channels assuming an expression ratio of a cassette of housekeeping genes to be 1. This step was essential because of differences in the fluorescent efficiencies of the dyes and because of differences in the efficiency with which the RT enzyme incorporates them into cDNA. In practice: (a) the statistical distribution of the expression ratios of all housekeeping genes was determined; (b) for those housekeeping genes with expression ratios within 1 standard deviation (SD) of the mean, a correction factor for the Cy3 intensity values was determined to force their average expression ratio to 1; and (c) this correction factor was then applied to all other fluorescence data from the microarray. (2) The second step was to determine the spots containing significant hybridization of both labeled cDNAs, so that an expression ratio could be calculated. The standard deviation of the mean of the log 10 of the ratios for the housekeeping genes was used to calculate 95% and 99% confidence intervals, against which the ratios of signal intensities from the Cy3 and Cy5 labels on each and every other spot on the chip were compared.

NIH microarray. The methodology for the analysis of cDNA microarray data has been reported previously in detail [19–21]. The quality of the hybridization in every spot of the NIH microarrays was rated from 0 (worse) to 1 (best) according to the intensity of fluorescence and area of the spot. Only hybridization ratios of 0.7 or more in the reciprocal arrays were considered for analysis of the expression ratios. A standard deviation of the variation in fluorescence intensity of the housekeeping

genes was calculated and applied to define differential expression of all other genes on the chips. An additional statistical analysis was calculated for the NIH microarray experiments based on the assumption that, in our experimental setting, the vast majority of the genes were expected to be expressed at a similar level in control and migration-activated cells [22]. The spots of the microarray with quality scores of 0.7 or more were selected for this analysis. The mean of the log 10 of all the ratios and its standard deviation were calculated. Outliers, that is genes with the strongest, reproducible differential expression, were identified.

For detailed information about the cDNA microarrays used for these experiments, the following web sites can be consulted: *http://microarray.azcc.arizona.edu/* and *http://www.nhgri.nih.gov/DIR/Microarray/main.html*.

Laser capture microdissection (LCM) of frozen glioblastoma specimens

Cryopreserved GBM specimens from three patients were cut in serial 6 μm sections and mounted on uncoated slides treated with diethyl pyrocarbonate (DEPC). The tumor core and adjacent invasive rim were identified on a coverslipped section stained with hematoxylin and eosin (HE). Cryostat sections intended for LCM were transferred from −80°C storage, and immediately immersed in 75% ethanol at RT for 30 sec. Slides were rinsed in H_2O, stained with filtered Meyer's hematoxylin for 30 sec, rinsed in H_2O, stained with bluing reagent for 20–30 sec, washed in 70% and 95% ethanol for 1 min each, stained with eosin Y for 20–30 sec, and dehydrated in 95% ethanol (2×1 min), 100% ethanol (stored over molecular sieve) (3×1 min) and xylenes (3×10 min). Slides were air-dried under a laminar flow for 10–30 min and immediately processed for LCM. DEPC-treated, autoclaved, distilled water was used to prepare every solution.

LCM was performed with a PixCell II Microscope (Arcturus Engineering, CA) using a 7.5 μm laser beam at 50–60 mW. GBM cells in the tumor core were readily identified and captured. Tumor cells immediately adjacent to necrotic or cortical areas, cells with small regular nuclei, endothelial cells, and blood cells were avoided. Neoplastic astrocytes in the invasive rim about 1 cm from the edge of the tumor core were identified according to the criteria of nuclear atypia and, when possible, according to their nuclear and/or cytoplasmic similarity with the GBM cells in the core. Between 1000 and 2000 glioblastoma cells were captured from tumor core and invasive rim from each specimen.

Quantitative, real-time polymerase chain reaction for tenascin C

Using the StrataPrep® Kit (Stratagene®), total RNA was isolated from matched aliquots of culture cells (cell lines T98G and SF767) on ECM and plastic, as well as from tumor cells from the core and invasive edge of three human glioblastoma specimens. Reverse transcription was performed with the RETROscript™ Kit (Ambion®). Polymerase chain reaction for histone H3.3 (housekeeping gene used for normalization) and tenascin C (TnC) was performed for the matched cDNA samples using the LightCycler® (Roche®), which allows real-time monitoring of the increase in amplicon concentration after every cycle based on fluorescence of the dsDNA dye SYBRgreen [23,24]. The number of cycles necessary to produce a detectable amount of TnC product above background was recorded for the matched samples. After correction for the difference in cycle number for histone H3.3 between the matched samples, the ratio of expressed TnC from cells on ECM versus plastic, or from cells at the edge versus tumor core was calculated as $2^{(\text{difference in cycle number})}$, (Tables 5 and 6). Amplicon specificity was confirmed by analysis of the melting curve and agarose-gel electrophoresis (Figure 6).

Results

Human glioma cells respond to the glioma-derived substrate by markedly accelerated adhesion and migration (Figure 1). The cells show an early migration response soon after attachment to the substrate (typically within hours). Cell morphology on the biological substrate shows early development of a spread appearance, and prompt development of filopodia and lamelipodia. Cells cultivated on the glioma-derived matrix characteristically occupy more surface area, have longer cellular processes (Figure 2), and grow more slowly than cells on tissue culture plastic flasks.

AZCC microarray. The relative expression level could be calculated as a ratio ECM/plastic for about 3900

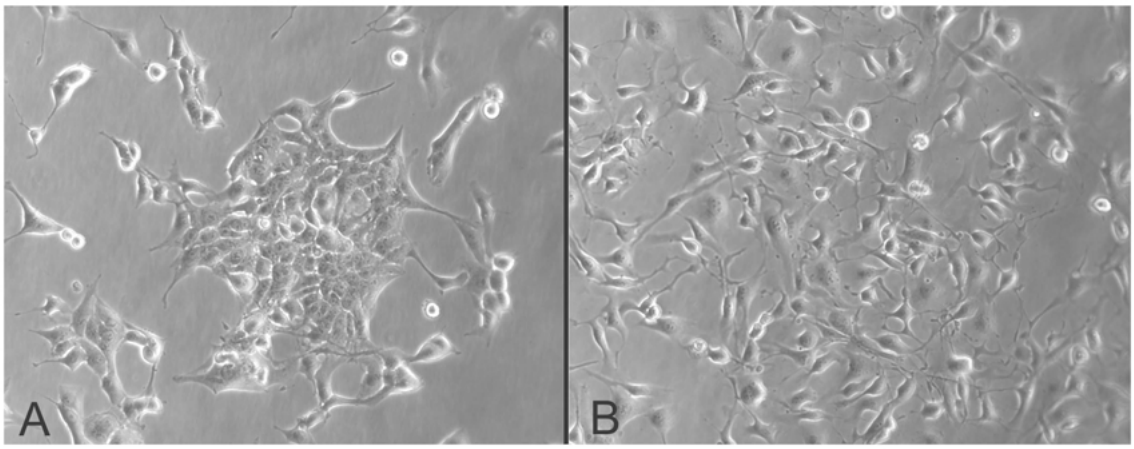

Figure 2. Morphology of G112 glioma cells on cell-derived ECM: (A) G112 cells seeded on untreated culture flask for approximately 72 h; (B) G112 cells seeded at the same time and in the same number on a culture flask coated with cell-derived ECM. On ECM, the area occupied by every cell, the number and length of filopodia, and the size of lamelipodia were larger than on uncoated flasks. Cells on plastic typically grew in groups and sheets whereas cells on ECM were more scattered throughout the available surrounding space.

gene sequences of the 5000 printed on the array. The correction factor to normalize the values of Cy3 to the Cy5 fluorescence was 1.28. The mean of all ratios was 0.83. The range within 1 SD was 0.45–1.2, 0.28–1.95 for 2 SD, and 0.17–3.18 for 3 SD. The number of genes calculated to be outliers according to these statistical criteria was 671, 67, and 4, respectively.

NIH microarray. Gene expression profiling was conducted in replicate using reciprocal fluorescent labeling of the two cDNA populations. Two ratios ECM/plastic, called NIH#1 and NIH#2, were calculated for each gene. Of the total 7000 genes on the array, a ratio NIH#1 and NIH#2 could be calculated for 3447 and 2733 genes, respectively. The standard deviations accounting for variations in fluorescent intensities for the housekeeping genes were 0.195 for the NIH#1 chip, and 0.184 for the NIH#2 chip. The mean ratio of genes with quality scores of 0.7 or greater was 1.11 for the NIH#1 chip, and 0.95 for the NIH#2 chip. The ranges within 1 SD were 0.63–1.93 for the NIH#1 chip, and 0.57–1.58 for the NIH#2 chip. The ranges within 2 SD were 0.36–3.37 for the NIH#1 chip, and 0.35–2.63 for the NIH#2 chip.

The relative expression ratios for genes involved in cell motility are shown in Table 1. Over expression by up to 4-fold was seen for tenascin C, neuropilin 2, GAP43, and PLCgamma2. Twenty other genes in migration-activated glioma cells up regulated by 1.3–4-fold are shown in Table 1. Fifteen genes down regulated in migrating glioma cells are also listed in Table 1; these were between 0.15 and 0.8 times at lower intensities than the same glioma cells on a substrate of tissue culture plastic. Notably, TPA, profilin, gelsolin, TIMP2, and several integrin subunits were expressed in lesser amounts in migrating cells. Integration of these migration mediators into the scheme of cell motility is portrayed in Figure 3.

Seventeen genes with putative roles in apoptosis which were up regulated and 20 genes down regulated in the migrating glioma cells are shown in Table 2. Cell survival genes such as Bcl-2 family members are over expressed in migration-activated cells, while mediators of the intrinsic apoptosis pathway, caspase 9, or the extrinsic apoptosis pathway, Sentrin, FADD, and caspase 8, are strongly down regulated. A schematic flowchart of the cell death machinery and the changes in gene expression of the various mediators are illustrated in Figure 4. The overall outcome to the gene expression changes of these factors is a reduced capacity of the cells to undergo programmed cell death.

Table 3 lists cell cycle regulators that showed consistent changes in expression when glioma cells were activated to migrate. TGFbeta2 and insulin-like growth factor 1 receptor were over expressed in the migrating cells by 5- and ∼3-fold, respectively. A large number (26) of genes with demonstrated activity in promoting

Table 1. Relative expression levels for motility-associated genes

Clone ID	Clone title	Ratio ECM/plastic		
		NIH#1	NIH#2	AZCC
Up regulated on ECM				
23185	Hexabrachion (tenascin C, cytotactin)	**4.83**	**4.93**	0.61
269354	Neuropilin 2	**4.15**	**6.58**	N/A
44563	Growth-associated protein 43	**4.48**	**3.89**	0.64
204897	Phospholipase C, gamma 2 (phosphatidylinositol-specific)	**4.76**	**3.92**	**1.76**
269354	Neuropilin 2	**3.95**	**3.73**	N/A
713145	CD44 antigen (homing function and Indian blood group system)	**3.88**	**3.53**	**2.00**
884783	PTPL1-associated Rho GAP1	**3.13**	**3.27**	N/A
135791	FN-14 (fibroblast growth factor inducible)	**3.00**	**4.30**	L/F
214982	MSE55	**2.90**	**2.50**	NA
378461	Osteopontin (secreted phosphoprotein I)	**2.74**	**3.00**	N/A
49389	Syntaxin 1 A	**2.60**	**2.25**	N/A
251019	Cadherin E	**2.80**	**2.30**	**1.90**
810934	Elastin	L/F	L/F	**2.73**
898092	Connective tissue growth factor	**2.58**	**2.27**	**1.37**
244307	Plasminogen activator inhibitor type 1 (PAI-1)	**2.44**	**2.10**	1.00
208718	Annexin 1 (lipocortin 1)	**2.00**	**2.17**	0.63
110467	Caveolin 2	**1.87**	**1.90**	**2.92**
281978	ras-relat. C3 bot. toxin substrate 3 (rho family, small GTP binding protein Rac3)	**1.40**	1.14	**1.71**
37491	Homo sapiens mRNA for Cdc42-interacting protein 4 (CIP4)	**1.53**	**1.54**	N/A
232826	Arp2/3 protein complex subunit p21	**1.36**	1.13	**1.56**
324861	EGFR (avian erythroblastic leukemia viral (v-erb-b) oncogene homolog)	**1.30**	**1.79**	L/F
131362	Moesin	**1.36**	**1.34**	**1.40**
755145	Villin 2 (ezrin)	**1.26**	**1.22**	1.09
755612	G-protein-coupled receptor 39	**1.29**	**1.23**	N/A
Down regulated on ECM				
796323	Adducin 3 (gamma)	**0.15**	**0.19**	NA
813841	Tissue plasminogen activator	**0.21**	**0.43**	0.70
773286	Solute carrier family 9 (sodium/hydrogen exchanger), isoform 3 regulatory factor 1	**0.20**	**0.20**	NA
365060	rab11A, member of ras oncogene family	**0.35**	**0.43**	0.50
486110	Profilin 2	**0.42**	**0.48**	NA
214900	Gelsolin	**0.45**	**0.47**	**0.36**
755952	Plexin 5	**0.51**	**0.63**	NA
245422	Adducin 1 (alpha)	**0.56**	**0.58**	LF
343072	Human beta-1D integrin mRNA, cytoplasmic domain, partial cds	**0.56**	**0.65**	0.84
204257	A disintegrin and metalloprotease domain 9 (meltin gamma)	**0.47**	**0.66**	NA
842846	Tissue inhibitor of matrix metalloprotease 2	**0.66**	**0.58**	NA
377671	Integrin, alpha 7	**0.57**	0.82	NA
212078	Integrin, alpha 1	**0.65**	0.89	NA
246786	Human orphan G-protein-coupled receptor (RDC1) mRNA, partial cds	**0.70**	**0.64**	LF
824426	Human PDGF associated protein mRNA, complete cds	**0.80**	0.88	NA

The ratio ECM/plastic is indicated for the three experiments NIH#1, NIH#2, and AZCC. Values greater than 1 indicated relative over expression in cells seeded on the motility-enhancing substrate (cell-derived ECM), whereas values smaller than 1 indicate relative under expression in those cells. Ratios in bold indicate a significance level of more than 1 SD (variation of fluorescence) outside the normalized housekeeping genes. L/F denotes low fluorescence, meaning that the ratio could not be interpreted (see Methods). N/A denotes that the gene was not present on this microarray.

the cell cycle were found to be under expressed in the migrating cells compared to cells on a non-motile substrate. This large list of factors is partially integrated into a scheme of cell proliferation in Figure 5. In general, the changes in expression levels of these genes would render the cell population less active in its cell cycle.

Sixty-four known genes or ESTs whose expression levels differed by at least 2 SD from the mean of all candidate cDNA probes of high quality in the three

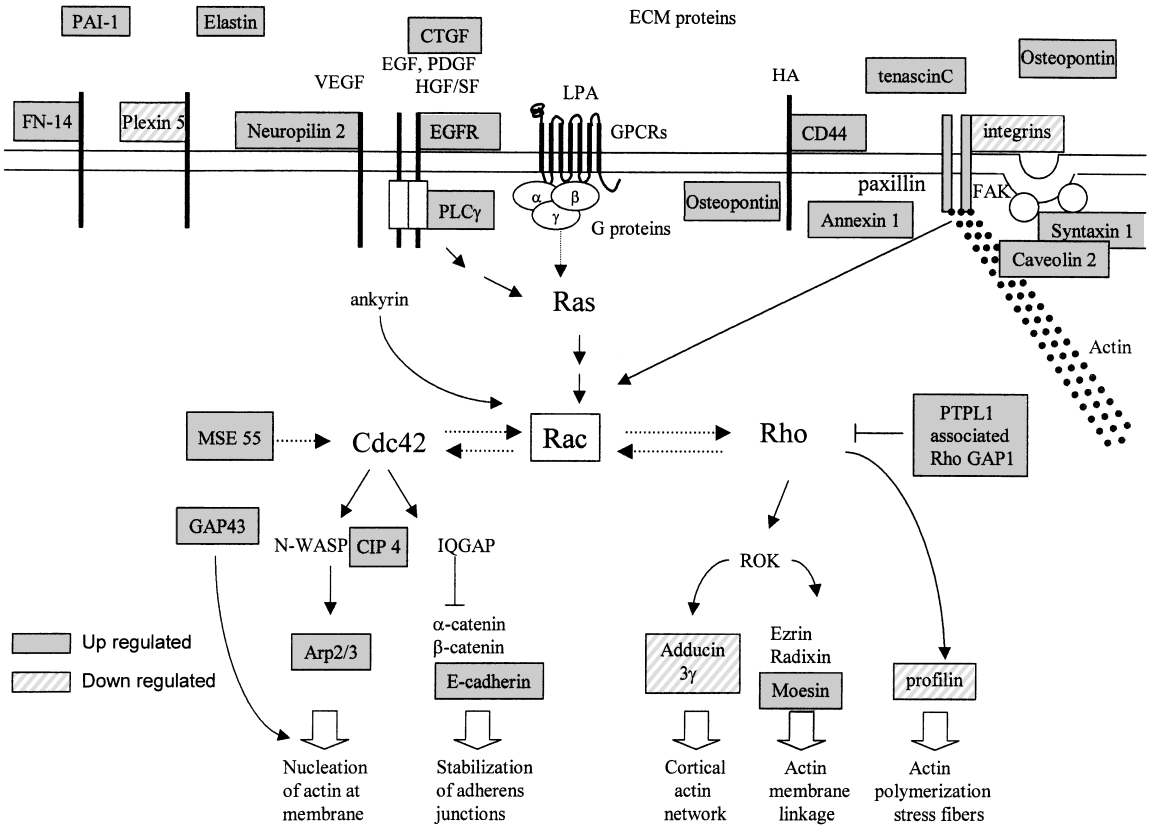

Figure 3. Generalized schemes for regulation of glioma cell migration (adapted from [57–60]). Genes up regulated in the G112 migration-stimulated cells are highlighted in gray boxes while those down regulated under migrating conditions are in the shaded boxes.

microarrays are listed in Table 4. This list conveys those genes and ESTs most dramatically regulated during the migrating phenotype. Nineteen of these genes are up regulated, and 45 are down regulated when glioma cells are activated to migrate. The biological or pathological significance of these genes, such as crystallin alpha B (up regulated) and crystallin mu (down regulated), or uridine phosphorylase and metallothioneins is undetermined at present. Other genes strongly down regulated include alpha-2-macroglobulin, carbonic anhydrase II, and a v-fos homolog, whose roles in glioma behavior or in cell motility are unknown.

Since tenascin C was up regulated in actively migrating G112 glioma cells, similar studies in two additional glioma cell lines were conducted (Table 5). Both T98G and SF767 up regulated tenascin C expression coincident to activated migration. Evaluation of the tenascin C mRNA levels of human glioma cells *in situ* captured by LCM from biopsy specimens revealed a marked disparity in levels of expression between the tumor core glioma cells relative to the invasive rim (Table 6). In two of the three specimens examined, mRNA for tenascin C could only be detected in the invasive rim cells, and was absent in the core glioma cells. PCR products were verified by melting curve analysis and by agarose-gel electrophoresis (Figure 6). (Specific isolation of endothelial cells at the invasive rim also demonstrated tenascin C mRNA, but at much lower levels than in the invading glioma cells (data not shown).)

Discussion

Differential expression of motility-related genes on cell-derived ECM

Although the migration response of the G112 glioma cells is prompt, adjustments in the gene expression profile would likely sustain the heightened

Table 2. Relative expression levels for apoptosis-regulatory genes

Clone ID	Clone title	Ratio ECM/plastic		
		NIH #1	NIH #2	AZCC
Up regulated on ECM				
814478	Bcl-2-related protein A1	L/F	L/F	**2.87**
841357	'DNA fragmentation factor, 45 kD, alpha subunit'	**2.43**	**2.56**	**1.94**
345858	'Human cisplatin resistance assocated beta protein (hCRA beta) mRNA'	**1.84**	**2.16**	L/F
208718	Annexin I (lipocortin I)	**2.07**	**2.16**	0.63
755506	Annexin IV (placental anticoagulant protein II)	**1.72**	**1.76**	0.29
82556	'Cytochrome p450 oxyreductase (human, placenta, mRNA partial, 2403 nt)'	**1.36**	**1.87**	**1.23**
795543	'Human antioxidant enzyme AOE37-2 mRNA, complete cds'	**1.7**	**1.47**	N/A
235938	Bcl-2-antagonist/killer 1	**1.42**	**1.59**	N/A
1486083	'Interleukin 1, alpha'	L/F	L/F	**1.41**
755301	'Homo sapiens mRNA for protein kinase C delta-type, complete cds'	**1.28**	**1.26**	**1.45**
135247	Inhibitor of protein kinase PKR	**1.33**	**1.27**	N/A
241481	'Caspase 10, apoptosis-related cysteine protease'	**1.31**	**1.28**	L/F
810039	Defender against cell death 1	**1.26**	**1.24**	L/F
795729	Bcl-2-antagonist of cell death	1.16	1.18	L/F
72778	'Caspase 7, apoptosis-related cysteine protease'	1.03	**1.22**	**1.27**
786680	Annexin V (endonexin II)	1.16	**1.26**	N/A
625584	TRAF interacting protein	1.11	1.16	N/A
Down regulated on ECM				
366971	Topoisomerase (DNA) II alpha (170 kD)	**0.05**	**0.09**	N/A
714213	'Tumor necrosis factor receptor superfamily, member 6'	**0.24**	L/F	L/F
489489	Lamin B receptor	**0.32**	**0.35**	L/F
345586	'Tumor necrosis factor receptor superfamily, member 12'	**0.35**	L/F	L/F
323500	'Caspase 6, apoptosis-related cysteine protease'	**0.38**	L/F	0.49
897544	Lamin A/C	**0.42**	L/F	0.75
214990	'Gelsolin (amyloidosis, Finnish type)'	**0.46**	**0.47**	1.98
309776	CASP8 and FADD-like apoptosis regulator	**0.5**	L/F	N/A
813714	CASP8 and FADD-like apoptosis regulator	**0.52**	L/F	N/A
1468461	Annexin XIII	**0.61**	L/F	N/A
843094	Ubiquitin-like 1 (sentrin)	**0.61**	**0.62**	0.6
76362	'Spectrin, alpha, non-erythrocytic 1 (alpha-fodrin)'	**0.62**	**0.64**	0.6
24032	CASP2 and RIPK1 domain containing adaptor with death domain	**0.71**	L/F	L/F
429574	'Caspase 3, apoptosis-related cysteine protease'	**0.73**	L/F	**0.38**
813166	TNF receptor-associated factor 6	**0.75**	L/F	0.74
789357	Nuclear factor of kappa light polypeptide gene enhancer in B-cells 1 (p105)	**0.76**	**0.61**	0.96
429574	'Caspase 3, apoptosis-related cysteine protease'	**0.78**	L/F	**0.38**
705110	'Caspase 9, apoptosis-related cysteine protease'	0.81	L/F	N/A
841292	Ubiquitin-conjugating enzyme E2I (homologous to yeast UBC9)	0.85	L/F	L/F
502486	'Human TRAF-interacting protein I-TRAF mRNA, complete cds'	0.87	L/F	N/A

The derivation of the ratios is as described in Table 1.

motility. A generalized scheme of the mediators of cell migration is shown (Figure 3), and different candidate factors present on the cDNA microarray chips were evaluated for differential expression between the parental and migration-activated cells (Table 1). A central regulator of actin nucleation at the leading edge of a migrating cell is Cdc42 [25]. Although Cdc42 is not elevated in the G112 cells on ECM, there is a heightened expression of both MSE55 and rac, which activate Cdc42 [25,26]. Cdc42 acts via N-WASP and CIP4 [27], of which CIP4 is over expressed in the migration-stimulated cells. CIP4 functions to localize N-WASP to microtubules, facilitating binding to Arp2/3, promoting actin polymerization at the membrane [28]; Arp2/3 is also up regulated in migrating glioma cells. Actin nucleation is also fostered by GAP43 [29], found to be over expressed in the migration-selected glioma cells; GAP43 action is triggered via protein kinase C, likely associated with receptor tyrosine kinases [30]. This

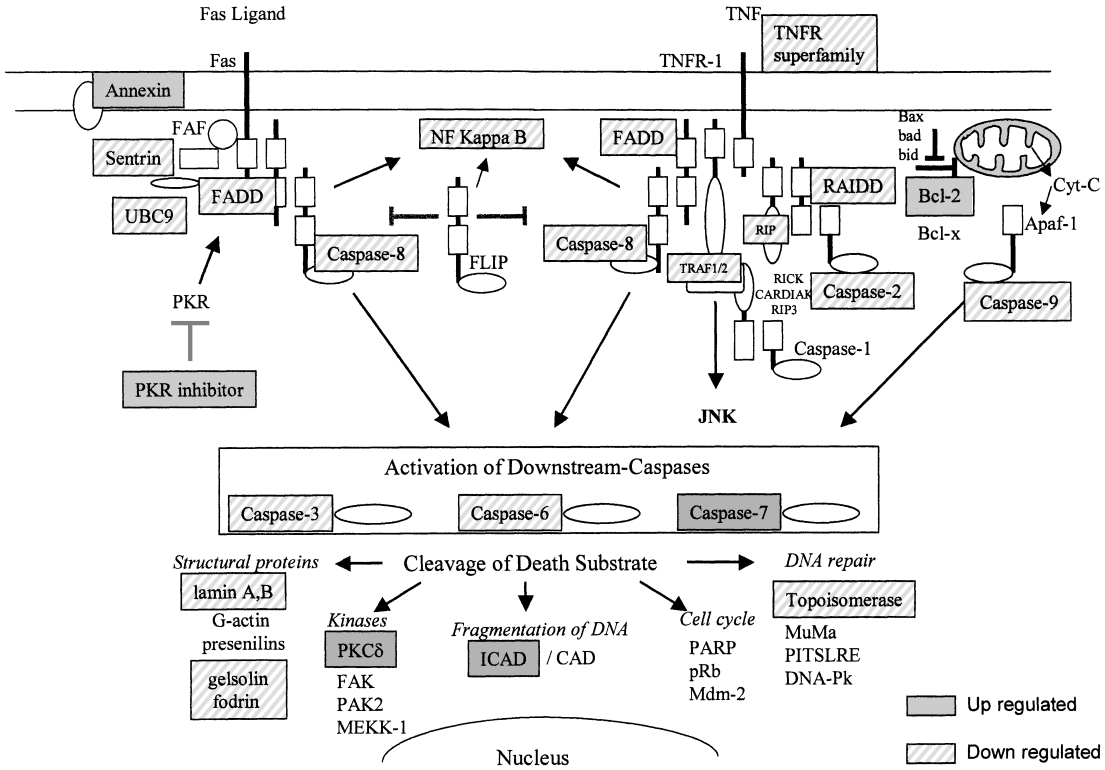

Figure 4. Generalized scheme for regulation of the programmed cell death (apoptosis) pathways (adapted from [54] and Alexis® Biochemicals). Genes up regulated in the G112 migration-stimulated cells are highlighted in gray boxes while those down regulated under migrating conditions are in the shaded boxes.

concert of up regulated genes argues for a net activation of actin nucleation, which is necessary for cell migration.

Further upstream from the biomechanics of motility is Rho, which is a regulator of rac activity [25]. Rho is also inhibited by PTPL1-associated Rho GAP1 (PARG1) [31] which is up regulated. Adducin 3γ [32–34] was one of the strongest down regulated migration-associated genes. The net outcome of the changes in Rho-regulated genes would be a reduced capacity to develop cell anchors with the matrix, consistent with a heightened motility tendency [35].

The cDNA microarray candidate genes involved in signaling cell motility include receptor tyrosine kinases such as EGFR [36] as well as neuropilin 2 (which is a receptor associated with neuronal axon guidance in development [37] and mediates proliferation and motility signaling by splice variants of VEGF [38,39]), which are up regulated in the migrating cells. Similarly, PLCgamma is strongly up regulated in the migrating glioma cells. These signaling mediators reside far upstream in cascades that impact cell migration and proliferation.

The expression of G-protein-coupled receptors (GPCRs) and integrins (α1, α7, and β1D) was down regulated in the migrating glioma cells. Some of these genes showed the largest levels of inactivated expression (Table 1). Witkowski et al. [40] report that shortened integrin half-life levels (possibly related to down regulation of integrin expression) are associated with accelerated motility of cells. Concomitantly, different receptors and matrix factors characteristically associated with accelerated motility are found to be up regulated by the migration-activated glioma cells. These include CD44 [41,42], osteopontin [43], annexin 1 [44], TnC [45], FN-14 [46], elastin [47], and CTGF [48]. The analysis by QRT-PCR confirmed over expression of TnC in two additional cell lines (SF767 and T98G) with stimulated motility and in invasive glioblastoma cells in three human specimens '*ex vivo*' (Tables 5 and 6, Figure 6). Up regulation of caveolin 2 [49] and syntaxin 1 [50] are likely related to

Table 3. Relative expression levels for cell-cycle regulatory and cytokine genes

Clone ID	Clone title	Ratio ECM/plastic		
		NIH#1	NIH#2	AZCC
Up regulated on ECM				
666218	'Transforming growth factor, beta 2'	L/F	**5.03**	L/F
682555	Insulin-like growth factor 1 receptor	F/L	F/L	**2.86**
Down regulated on ECM				
950690	Cyclin A2	**0.09**	**0.02**	0.65
898286	'Homo sapiens mRNA for CDC2 delta T, complete cds'	**0.11**	**0.18**	0.53
291057	'Cyclin-dependent kinase inhibitor 2C (p18, inhibits CDK4)'	**0.14**	**0.19**	N/A
768370	'ras homolog gene family, member B'	**0.15**	**0.13**	0.69
435076	Centromere protein F (400 kD)	**0.154**	**0.36**	N/A
742798	'Homo sapiens mitotic centromere-associated kinesin mRNA, complete cds'	**0.159**	**0.16**	N/A
814701	'MAD2 (mitotic arrest deficient, yeast, homolog)-like 1'	**0.18**	L/F	**0.37**
769921	'Human cyclin-selective ubiquitin carrier protein mRNA, complete cds'	**0.19**	**0.17**	**0.45**
36374	Cyclin B1	**0.24**	**0.52**	N/A
789182	Proliferation nuclear cell antigen (PCNA)	**0.28**	**0.29**	0.54
700792	Cyclin-dependent kinase inhibitor 3 (CDK2-assoc. dual specificity phosphatase)	**0.32**	**0.41**	N/A
365060	'rab11A, member ras oncogene family'	**0.33**	**0.43**	0.52
68950	Cyclin E1	**0.33**	LF	N/A
773599	Retinoblastoma-binding protein 4	**0.41**	**0.41**	**0.44**
1055753	Tumor protein p53-binding protein	**0.45**	L/F	N/A
296095	'Homo sapiens E2F-related transcription factor (DP-1) mRNA, complete cds'	**0.47**	**0.47**	N/A
783729	v-erb-b2 avian erythroblastic leukemia viral oncogene homolog 2	**0.55**	**0.64**	F/L
133972	'rab2, member ras oncogene family'	**0.60**	**0.74**	0.51
250667	'rab9, member ras oncogene family'	**0.65**	LF	**0.43**
768260	E2F transcription factor 1	**0.66**	**0.70**	N/A
827013	'Tumor protein 53-binding protein, 1'	**0.68**	**0.96**	**0.39**
293715	'rab1, member ras oncogene family'	**0.70**	**0.78**	0.73
321189	rap1B, member of ras oncogene family	**0.72**	**1.08**	**0.34**
141768	v-erb-b2 avian erythroblastic leukemia viral oncogene homolog 2	**0.73**	**0.73**	0.67
280752	Retinoblastoma-like 2 (p130)	**0.80**	L/F	L/F
842806	Cyclin-dependent kinase 4	0.88	**0.75**	0.58

The derivation of the ratios is as described in Table 1.

the robust demands for cell membrane turnover (synthesis and resorption) coincident to accelerated motility. Lastly, plasminogen activator inhibitor-1 (PAI-1) is over expressed in the migrating glioma cells, consistent with several reports describing a role of plasminogen and PAI-1 dynamics in turnover of the ECM during cell invasion [51–53].

Down regulation of apoptotic pathways on cell-derived ECM

An overview of the main apoptotic pathways and of the relative expression levels of genes involved in these cascades is shown in Figure 4. Many of the listed genes encoding activator proteins of programmed cell death were down regulated in cells exposed to cell-derived ECM. The main effector caspases, caspase 3 and 6, were consistently reduced by 1.3–2.6-fold in cells exposed to ECM. Upstream of the effector caspases, initiator caspases were also down regulated. The relative level of caspase 8, an initiator caspase activated through Fas and TNFR signaling, was reduced by about 2-fold in ECM-exposed cells. Fas itself could not be interpreted because the hybridization failed on both arrays; members of the TNFR superfamily (initiators of the so-called extrinsic apoptotic pathway [54] were down regulated by about 3–4-fold on ECM. Of the mediators linked to the intrinsic, or mitochondrial, apoptotic cascade, only the inhibitor Bcl-2 was slightly up regulated, and the initiator caspase 9 was slightly down regulated on ECM. Changes in expression of other mediators of the intrinsic apoptosis pathway could not be interpreted from the microarray data. Data reflecting expression of Bax and cytochrome C were inconsistent among and within the same array.

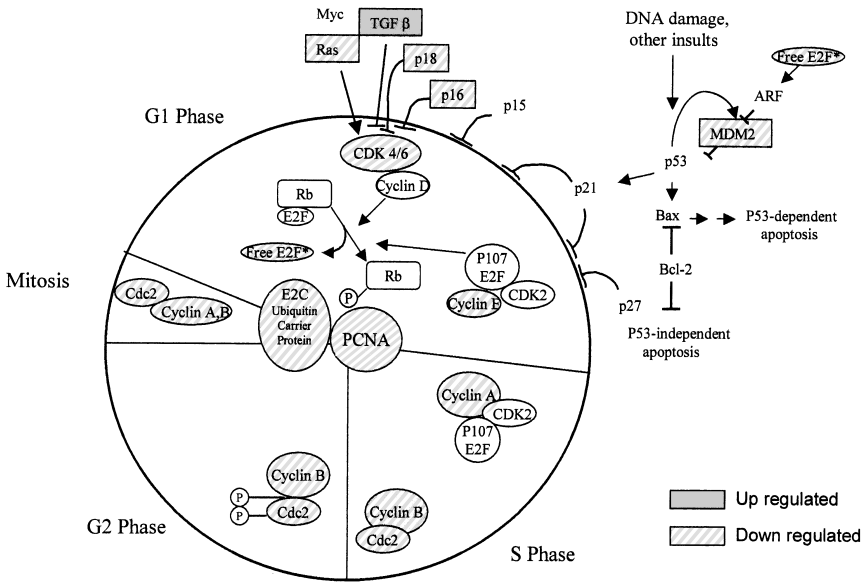

Figure 5. Generalized scheme for regulation of the cell cycle (adapted from [61]). Genes up regulated in the G112 migration-stimulated cells are highlighted in gray boxes while those down regulated under migrating conditions are in the shaded boxes.

Table 4. Listing of most differentially expressed genes from control versus migration-activated glioma cells

Chr. loc.	Clone ID	Clone title	Ratio ECM/plastic		
			NIH #1	NIH #2	AZCC
Up regulated on ECM					
11p13	713145	CD44 antigen (homing function and Indian blood group system)	**3.88**	**3.53**	**2.00**
	135791	Fn 14 for type 1 transmembrane protein	**3.03**	**4.35**	**2.66**
11q22.3	839736	'Crystallin, alpha B'	5.03	4.81	1.56
	300137	'Protein kinase, AMP-activated, beta 2 non-catalytic subunit'	6.21	7.35	N/A
	140337	ESTs	4.76	4.72	N/A
7.00	489677	Uridine phosphorylase	4.17	4.61	N/A
2q34	269354	Neuropilin 2	4.15	6.58	N/A
17p13	739183	CD68 antigen	3.48	4.33	L/F
	626716	ESTs	3.40	4.24	N/A
16q13	214162	Metallothionein 1H	3.32	4.17	L/F
	108316	rab3A interacting protein (rabin3)-like 1	3.26	3.79	L/F
	884783	PTPL1-associated Rho GAP1	3.13	3.27	N/A
16q13	202535	Metallothionein 1G	3.12	3.26	N/A
	725672	'Human transducin-like protein mRNA, complete cds'	3.10	2.95	N/A
	247635	Homo sapiens cDNA: FLJ23201 fis, KAIA38872	3.08	2.90	L/F
	232586	EST	2.94	2.94	N/A
	301122	'Human extracellular matrix protein 1 mRNA, alt. splice variant, cds'	2.92	3.85	L/F
	784065	'Homo sapiens Hsp89-alpha-delta-N mRNA, complete cds'	2.90	3.82	N/A
8q24.12	812965	v-myc avian myelocytomatosis viral oncogene homolog	2.78	3.00	L/F
Down regulated on ECM					
16p	42373	'Crystallin, mu'	**0.03**	**0.05**	**0.09**
	759865	'Human prepromultimerin mRNA, complete cds'	**0.05**	**0.10**	**0.18**
12p13.3	44180	Alpha-2-macroglobulin	**0.14**	**0.15**	**0.17**

Table 4. (Continued)

Chr. loc.	Clone ID	Clone title	Ratio ECM/plastic		
			NIH#1	NIH#2	AZCC
4q34	784910	Glycoprotein M6A	**0.16**	**0.22**	**0.24**
13q22	49665	Endothelin receptor type B	**0.19**	**0.35**	**0.10**
8q22	51865	Carbonic anhydrase II	**0.20**	**0.15**	**0.23**
	245860	Homo sapiens mRNA: cDNA DKFZp564H1916	**0.29**	**0.36**	**0.27**
	773254	Splicing fact. proline/glutam. rich (polypyr. tract-bind. protein-ass.)	0.29	0.27	0.21
2qter	341310	Frizzled-related protein	0.10	0.13	0.31
	211758	Homo sapiens cDNA: FLJ22256 fis, clone HRC02860	0.15	0.19	0.32
14q24.3	811015	v-fos FBJ murine osteosarcoma viral oncogene homolog	0.28	0.34	0.62
7q11.23	548957	'General transcription factor II, i, pseudogene 1'	0.29	0.33	0.46
5q31	415102	Cell division cycle 25C	0.04	0.09	N/A
17q21	366971	Topoisomerase (DNA) II alpha (170 kD)	0.05	0.09	N/A
6p21.3	1461138	'H4 histone family, member G'	0.06	0.27	N/A
14q21	855910	'Lectin, galactoside-binding, soluble, 3 (galectin 3)'	0.08	0.09	N/A
19p13.1	309515	Cartilage oligomeric matrix protein	0.09	0.18	N/A
5q31.1	840944	Early growth response 1	0.11	0.11	N/A
	744047	Polo (Drosophia)-like kinase	0.11	0.14	N/A
	490995	ESTs	0.12	0.17	N/A
2q14	781047	Budding uninhibited by benzimidazoles 1 (yeast homolog)	0.12	0.23	N/A
1q42.1	340657	'Endometr. bleed. ass. factor (factor A; TGF beta superfamily)'	0.14	0.33	N/A
18q21.1	854581	Transcription factor 4	0.14	0.19	N/A
1p32	291057	'Cyclin-dependent kinase inhibitor 2C (p18, inhibits CDK4)'	0.14	0.19	N/A
15q23	236333	Immunoglobulin superfamily containing leucine-rich repeat	0.15	0.23	N/A
10q24.2	796323	Adducin 3 (gamma)	0.15	0.19	N/A
17q23.2	379920	'Thymidine kinase 1, soluble'	0.15	0.12	N/A
1q32-q41	435076	Centromere protein F (400 kD)	0.15	0.36	N/A
	42864	EST	0.15	0.25	N/A
	742798	'Homo sapiens mitotic centromere-ass. kinesin mRNA, cds'	0.16	0.16	N/A
17p13.1	531319	Serine/threonine kinase 12	0.17	0.17	N/A
12p13.3	878182	Alpha-2-macroglobulin	0.17	0.21	N/A
	773286	'Solute carrier family 9 (sodium/hydrogen exch.), isoform 3 reg. factor 1'	0.20	0.20	N/A
	213136	'Human BTG2 (BTG2) mRNA, complete cds'	0.20	0.36	N/A
7q32	290378	Podocalyxin-like	0.22	0.34	N/A
17p13.3	878178	'Platelet-activat. factor acetylhydrolase, isoform Ib, alpha subunit (45 kD)'	0.23	0.32	N/A
	744800	Protein tyrosine phosphatase J	0.26	0.25	N/A
17.00	383188	Recoverin	0.26	0.30	N/A
1p35-36.1	1476065	Leukemia-associated phosphoprotein p18 (stathmin)	0.26	0.20	N/A
16p13.3	455128	Cyclin F	0.26	0.29	N/A
17q11-qter	810711	Cytochrome b-561	0.26	0.28	N/A
19.00	857319	'Eukaryotic translation initiation factor 3, subunit 4 (delta, 44 kD)'	0.26	0.22	N/A
	725877	'Creatine transporter (human, brainstem/spinal cord, mRNA, 2283 nt)'	0.27	0.29	N/A
	249603	ESTs	0.27	0.28	N/A
12.00	756687	'CD36 antigen (collagen type I receptor, thrombospondin receptor)-like 1'	0.27	0.28	N/A
	725877	'Creatine transporter (human, brainstem/spinal cord, mRNA, 2283 nt)'	0.28	0.28	N/A
22q11.2	453107	'Cdc45 (cell division cycle 45, S.cerevisiae, homolog)-like'	0.29	0.31	N/A

All differentially expressed genes were outliers from the mean of all ratios by more than 2 SD in at least two of the three experiments. In bold are the outliers by more than 2 SD in all three experiments. The boxed areas indicate outliers by more than 2 SD in two and 1 SD in the third experiment. L/F denotes low fluorescence, meaning that the ratio could not be interpreted (see Methods). N/A denotes that the gene was not present on this microarray.

Other potentially interesting genes, like Apaf-1, were not printed on the arrays. Overall, the data were consistent with a gene expression profile resulting in increased apoptotic resistance in cells with induced motility phenotype.

Table 5. Over expression of tenascin C by migration-stimulated T98G and SF767 cells

	T98G		SF767	
	Plastic	ECM	Plastic	ECM
Cycle no. histone (Hist.)	15.51	15.59	14.68	14.78
Difference in cycle no. (Hist.)		0.08		0.1
Cycle no. tenascin C (TnC)	32.88	21.44	26.71	25.47
Difference in cycle no. (TnC)	11.44		1.24	
Net difference in favor of migrating cells		11.36		1.23
Fold over expression of TnC on ECM		2628.5		2.3

The glioma cell lines T98G and SF767 were seeded either on plain culture flasks or on cell-derived ECM, a motility-enhancing substrate. The relative expression levels of tenascin C (TnC) on ECM versus plastic were calculated using real-time RT-PCR after normalization of the samples to histone H3.3. TnC was over expressed in both cell lines when motility was induced by ECM.

Down regulation of genes driving progression through the cell cycle

The gene encoding for proliferating cell nuclear antigen (PCNA), which is a typical marker of cell-cycle activity, was reduced by 2–3.5-fold in cells exposed to ECM. Another mRNA, encoding the human cyclin-selective ubiquitin carrier protein (E2C), which is ubiquitous throughout the cell cycle and catalyzes cells cycle progression [55], was also down regulated by 2–5.5-fold in the cell population with induced-motility phenotype. The same was true for the mitotic arrest deficient gene (MAD2L1), a mitotic spindle checkpoint, and the centromere protein F, which both indirectly reflect the mitotic activity of the cell [56]. These genes were down regulated by 2.5–5.5-fold in cells exposed to ECM. All the cyclins that were present on the arrays and were interpretable in terms of quality and consistency (cyclin A2, B1, E1, and Cdc2) were strongly down regulated by 3–50-fold in the cell population with the induced-motility phenotype. The level of expression of cyclin dependent kinase 4 (CDK4) was also slightly reduced in those cells while tumor growth factor beta 2 (TGFβ2), a CDK4 inhibitor, was strongly up regulated in motile cells. The relative expression levels of two other important positive cell-cycle regulators, E2F and MDM2 (p53 binding-protein), were also reduced (by 1.5–2-fold) in cells on ECM.

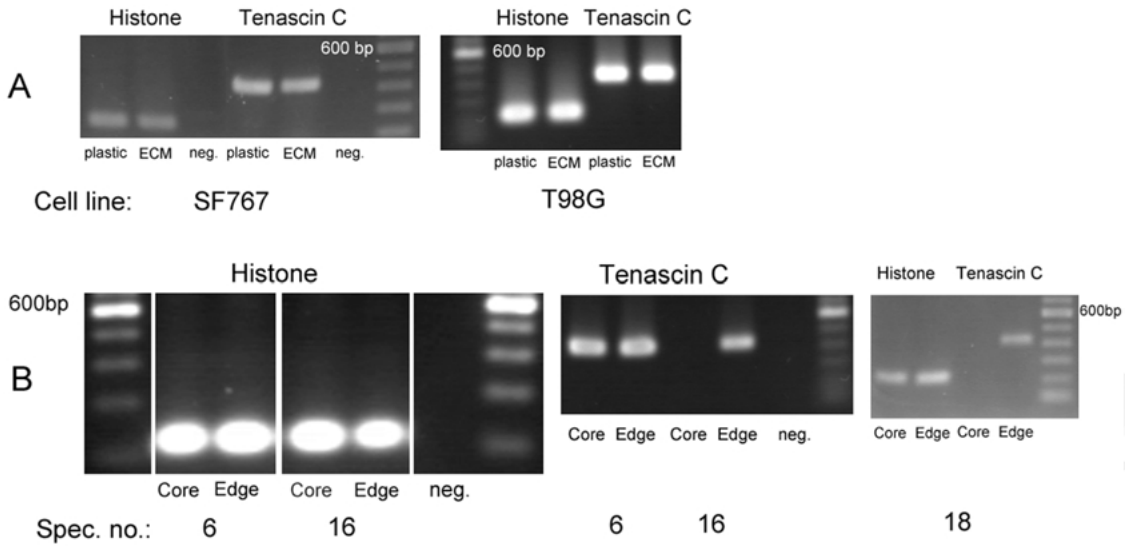

Figure 6. Confirmation of amplicon specificity for histone and TnC by agarose-gel electrophoresis. Agarose-gel electrophoresis showing PCR products of the expected size for histone H3.3 and tenascin C from the quantitative RT-PCR reactions reported in Table 5 (A) and in Table 6 (B).

Table 6. Over expression of tenascin C by invading glioblastoma cells '*ex vivo*'

	Specimen no. 6		Specimen no. 16		Specimen no. 18	
	Core	Edge	Core	Edge	Core	Edge
Cycle no. histone (Hist.)	25.46	24.2	26.32	27.97	22.71	21.74
Difference in cycle no. (Hist.)		1.26		1.65	0.97	
Cycle no. tenascin C (TnC)	35.88	33.94	No product	35.7	No product	33.11
Difference in cycle no. (TnC)	1.94		∞		∞	
Net difference in favor of the edge		0.68		∞		∞
Fold overexpression at the inv. edge		1.6		∞		∞

Tumor cells were harvested from the core and the invasive edge of three human glioblastoma specimens using LCM. The relative expression of TnC in the edge versus core samples was calculated using real-time RT-PCR after normalization to histone H3.3 as housekeeping gene. In specimens no. 16 and 18 TnC could be detected at the invasive edge only. In specimen no. 6 there was 1.6-fold over expression of TnC in invasive tumor cells.

Conclusion

Genetic profiling using cDNA microarrays is a powerful tool to discover some of the genetic determinants of the migratory/invasive phenotype and of complex cellular changes linked to motility. We provide evidence for an interdependence of motility, proliferation, and apoptosis at the transcription level in malignant glioblastoma cells. We found that stimulated migration is accompanied by a concomitant down regulation of genes responsible for proliferation and apoptosis. It is reasonable to speculate that therapeutic manipulations targeting the invasiveness of glioblastoma cells could have profound biological impact on collateral gene transcription in these cells, possibly making them more sensitive to cytotoxic treatments.

Acknowledgements

L. Mariani is funded by a Grant of the Swiss National Research Foundation. This work was supported by a grant from the Pediatric Brain Tumor Foundation of the United States. We are indebted to Javed Khan, at NHGRI, NIH, for his assistance in conducting the microarray experiments, and Rolf W. Seiler, Inselspital, Bern, Switzerland, for providing frozen GBM specimens.

References

1. Bittner M, Meltzer P, Chen Y, Jiang Y, Seftor E, Hendrix M, Radmacher M, Simon R, Yakhini Z, Ben Dor A, Sampas N, Dougherty E, Wang E, Marincola F, Gooden C, Lueders J, Glatfelter A, Pollock P, Carpten J, Gillanders E, Leja D, Dietrich K, Beaudry C, Berens M, Alberts D, Sondak V: Molecular classification of cutaneous malignant melanoma by gene expression profiling. Nature 406: 536–540, 2000
2. Chicoine MR, Silbergeld DL: The *in vitro* motility of human gliomas increases with increasing grade of malignancy. Cancer 75: 2904–2909, 1995
3. Giese A, Rief MD, Loo MA, Berens ME: Determinants of human astrocytoma migration. Cancer Res 54: 3897–3904, 1994
4. Berens ME, Rief MD, Loo MA, Giese A: The role of extracellular matrix in human astrocytoma migration and proliferation studied in a microliter scale assay. Clin Exp Metastasis 12: 405–415, 1994
5. Boudreau N, Bissell MJ: Extracellular matrix signaling: integration of form and function in normal and malignant cells. Curr Opin Cell Biol 10: 640–646, 1998
6. Enam SA, Rosenblum ML, Edvardsen K: Role of extracellular matrix in tumor invasion: migration of glioma cells along fibronectin-positive mesenchymal cell processes. Neurosurgery 42: 599–607, discussion 607–608, 1998
7. Sallinen SL, Sallinen PK, Haapasalo HK, Helin HJ, Helen PT, Schraml P, Kallioniemi OP, Kononen J: Identification of differentially expressed genes in human gliomas by DNA microarray and tissue chip techniques. Cancer Res 60: 6617–6622, 2000
8. Clark EA, Golub TR, Lander ES, Hynes RO: Genomic analysis of metastasis reveals an essential role for RhoC (see comments). Nature 406: 532–535, 2000
9. Dolan ME, Stine L, Mitchell RB, Moschel RC, Pegg AE: Modulation of mammalian O6-alkylguanine-DNA alkyltransferase *in vivo* by O6-benzylguanine and its effect on the sensitivity of a human glioma tumor to 1-(2-chloroethyl)-3-(4-methylcyclohexyl)-1-nitrosourea. Cancer Commun 2: 371–377, 1990
10. Marathi UK, Dolan ME, Erickson LC: Anti-neoplastic activity of sequenced administration of O6-benzylguanine, streptozotocin, and 1,3-bis(2-chloroethyl)-1-nitrosourea *in vitro* and *in vivo*. Biochem Pharmacol 48: 2127–2134, 1994
11. Giese A, Rief MD, Loo MA, Berens ME: Determinants of human astrocytoma migration. Cancer Res 54: 3897–3904, 1994

12. Gladson CL: The extracellular matrix of gliomas: modulation of cell function. J Neuropathol Exp Neurol 58: 1029–1040, 1999
13. Groth T, Altankov G, Kostadinova A, Krasteva N, Albrecht W, Paul D: Altered vitronectin receptor (alphav integrin) function in fibroblasts adhering on hydrophobic glass. J Biomed Mater Res 44: 341–351, 1999
14. Underwood PA, Bean PA, Mitchell SM, Whitelock JM: Specific affinity depletion of cell adhesion molecules and growth factors from serum. J Immunol Methods 247: 217–224, 2001
15. Akudugu JM, Slabbert JP, Serafin A, Bohm L: Frequency of radiation-induced micronuclei in neuronal cells does not correlate with clonogenic survival. Radiat Res 153: 62–67, 2000
16. Short S, Mayes C, Woodcock M, Johns H, Joiner MC: Low dose hypersensitivity in the T98G human glioblastoma cell line. Int J Radiat Biol 75: 847–855, 1999
17. Jones PA: Construction of an artificial blood vessel wall from cultured endothelial and smooth muscle cells. Proc Natl Acad Sci 76: 1882–1886, 1986
18. Vlodavsky I, Levi A, Lax I, Fuks Z, Schlessinger J: Induction of cell attachment and morphological differentiation in a pheochromocytoma cell line and embryonal sensory cells by the extracellular matrix. Dev Biol 93: 285–300, 1982
19. Heiskanen MA, Bittner ML, Chen Y, Khan J, Adler KE, Trent JM, Meltzer PS: Detection of gene amplification by genomic hybridization to cDNA microarrays. Cancer Res 60: 799–802, 2000
20. Khan J, Simon R, Bittner M, Chen Y, Leighton SB, Pohida T, Smith PD, Jiang Y, Gooden GC, Trent JM, Meltzer PS: Gene expression profiling of alveolar rhabdomyosarcoma with cDNA microarrays. Cancer Res 58: 5009–5013, 1998
21. Khan J, Bittner ML, Saal LH, Teichmann U, Azorsa DO, Gooden GC, Pavan WJ, Trent JM, Meltzer PS: cDNA microarrays detect activation of a myogenic transcription program by the PAX3-FKHR fusion oncogene. Proc Natl Acad Sci USA 96: 13264–13269, 1999
22. Duggan DJ, Bittner M, Chen Y, Meltzer P, Trent J M: Expression profiling using cDNA microarrays. Nat Genet 21: 10–14, 1999
23. Roche Biochemicals: LightCycler operators manual, version 3.0, 2000
24. Rasmussen RP, Morrison T, Herrmann M, Wittwer CT: Quantitative PCR by continuous fluorescence monitoring of a double strand DNA specific binding dye. Biochemica 2: 8–11, 1998
25. Schmitz AA, Govek EE, Bottner B, Van Aelst L: Rho GTPases: signaling, migration, and invasion (in process citation). Exp Cell Res 261: 1–12, 2000
26. Burbelo PD, Snow DM, Bahou W, Spiegel S: MSE55, a Cdc42 effector protein, induces long cellular extensions in fibroblasts. Proc Natl Acad Sci USA 96: 9083–9088, 1999
27. Tian L, Nelson DL, Stewart DM: Cdc42-interacting protein 4 mediates binding of the Wiskott–Aldrich syndrome protein to microtubules. J Biol Chem 275: 7854–7861, 2000
28. Prehoda KE, Scott JA, Dyche Mullins R, Lim WA: Integration of multiple signals through cooperative regulation of the N-WASP–Arp2/3 complex (in process citation). Science 290: 801–806, 2000
29. Maidment SL: The cytoskeleton and brain tumour cell migration. Anticancer Res 17: 4145–4149, 1997
30. Laux T, Fukami K, Thelen M, Golub T, Frey D, Caroni P: GAP43, MARCKS, and CAP23 modulate PI(4,5)P(2) at plasmalemmal rafts, and regulate cell cortex actin dynamics through a common mechanism. J Cell Biol 149: 1455–1472, 2000
31. Saras J, Franzen P, Aspenstrom P, Hellman U, Gonez LJ, Heldin CH: A novel GTPase-activating protein for Rho interacts with a PDZ domain of the protein-tyrosine phosphatase PTPL1. J Biol Chem 272: 24333–24338, 1997
32. Matsuoka Y, Li X, Bennett V: Adducin: structure, function and regulation. Cell Mol Life Sci 57: 884–895, 2000
33. Fukata Y, Oshiro N, Kinoshita N, Kawano Y, Matsuoka Y, Bennett V, Matsuura Y, Kaibuchi K: Phosphorylation of adducin by Rho-kinase plays a crucial role in cell motility. J Cell Biol 145: 347–361, 1999
34. Kimura K, Fukata Y, Matsuoka Y, Bennett V, Matsuura Y, Okawa K, Iwamatsu A, Kaibuchi K: Regulation of the association of adducin with actin filaments by Rho-associated kinase (Rho-kinase) and myosin phosphatase. J Biol Chem 273: 5542–5548, 1998
35. Hall A, Nobes CD: Rho GTPases: molecular switches that control the organization and dynamics of the actin cytoskeleton. Philos Trans Royal Soc Lond B Biol Sci 355: 965–970, 2000
36. Berens ME, Rief MD, Shapiro JR, Haskett D, Giese A, Joy A, Coons SW: Proliferation and motility responses of primary and recurrent gliomas related to changes in epidermal growth factor receptor expression. J Neuro-Oncol 27: 11–22, 1996
37. Chen H, Chedotal A, He Z, Goodman CS, Tessier-Lavigne M: Neuropilin-2, a novel member of the neuropilin family, is a high affinity receptor for the semaphorins Sema E and Sema IV but not Sema III. Neuron 19: 547–559, 1997
38. Handa A, Tokunaga T, Tsuchida T, Lee YH, Kijima H, Yamazaki H, Ueyama Y, Fukuda H, Nakamura M: Neuropilin-2 expression affects the increased vascularization and is a prognostic factor in osteosarcoma. Int J Oncol 17: 291–295, 2000
39. Gluzman-Poltorak Z, Cohen T, Herzog Y, Neufeld G: Neuropilin-2 and neuropilin-1 are receptors for the 165-amino acid form of vascular endothelial growth factor (VEGF) and of placenta growth factor-2, but only neuropilin-2 functions as a receptor for the 145-amino acid form of VEGF*. J Biol Chem 275: 18040–18045, 2000
40. Witkowski CM, Bowden GT, Nagle RB, Cress AE: Altered surface expression and increased turnover of the alpha6beta4 integrin in an undifferentiated carcinoma. Carcinogenesis 21: 325–330, 2000
41. Breyer R, Hussein S, Radu DL, Putz KM, Gunia S, Hecker H, Samii M, Walter GF, Stan AC: Disruption of intracerebral progression of C6 rat glioblastoma by *in vivo* treatment with anti-CD44 monoclonal antibody. J Neurosurg 92: 140–149, 2000
42. Gunia S, Hussein S, Radu DL, Putz KM, Breyer R, Hecker H, Samii M, Walter GF, Stan AC: CD44s-targeted treatment with monoclonal antibody blocks intracerebral

invasion and growth of 9L gliosarcoma. Clin Exp Metastasis 17: 221–230, 1999
43. Zohar R, Suzuki N, Suzuki K, Arora P, Glogauer M, McCulloch CA, Sodek J: Intracellular osteopontin is an integral component of the CD44–ERM complex involved in cell migration. J Cell Physiol 184: 118–130, 2000
44. Solito E, Romero IA, Marullo S, Russo-Marie F, Weksler BB: Annexin 1 binds to U937 monocytic cells and inhibits their adhesion to microvascular endothelium: involvement of the alpha 4 beta 1 integrin. J Immunol 165: 1573–1581, 2000
45. Phillips GR, Krushel LA, Crossin KL: Domains of tenascin involved in glioma migration. J Cell Sci 111 (Pt 8): 1095–1104, 1998
46. Meighan-Mantha RL, Hsu DK, Guo Y, Brown SA, Feng SL, Peifley KA, Alberts GF, Copeland NG, Gilbert DJ, Jenkins NA, Richards CM, Winkles JA: The mitogen-inducible Fn14 gene encodes a type I transmembrane protein that modulates fibroblast adhesion and migration. J Biol Chem 274: 33166–33176, 1999
47. Jung S, Hinek A, Tsugu A, Hubbard SL, Ackerley C, Becker LE, Rutka JT: Astrocytoma cell interaction with elastin substrates: implications for astrocytoma invasive potential. Glia 25: 179–189, 1999
48. Babic AM, Chen CC, Lau LF: Fisp12/mouse connective tissue growth factor mediates endothelial cell adhesion and migration through integrin alphavbeta3, promotes endothelial cell survival, and induces angiogenesis *in vivo*. Mol Cell Biol 19: 2958–2966, 1999
49. Mora R, Bonilha VL, Marmorstein A, Scherer PE, Brown D, Lisanti MP, Rodriguez-Boulan E: Caveolin-2 localizes to the golgi complex but redistributes to plasma membrane, caveolae, and rafts when co-expressed with caveolin-1. J Biol Chem 274: 25708–25717, 1999
50. Foletti DL, Lin R, Finley MA, Scheller RH: Phosphorylated syntaxin 1 is localized to discrete domains along a subset of axons. J Neurosci 20: 4535–4544, 2000
51. Chazaud B, Bonavaud S, Plonquet A, Pouchelet M, Gherardi RK, Barlovatz-Meimon G: Involvement of the [uPAR:uPA:PAI-1:LRP] complex in human myogenic cell motility. Exp Cell Res 258: 237–244, 2000
52. Liu Y, Honda S, Kohsaka S, Nakajima K: Plasminogen enhances the secretion of plasminogen activator inhibitor-1 from cultured rat astrocytes. Neurosci Lett 282: 137–140, 2000
53. Sugiura Y, Ma L, Sun B, Shimada H, Laug WE, Seeger RC, DeClerck YA: The plasminogen–plasminogen activator (PA) system in neuroblastoma: role of PA inhibitor-1 in metastasis. Cancer Res 59: 1327–1336, 1999
54. Reed JC: Mechanisms of apoptosis [in process citation]. Am J Pathol 157: 1415–1430, 2000
55. Townsley FM, Aristarkhov A, Beck S, Hershko A, Ruderman JV: Dominant-negative cyclin-selective ubiquitin carrier protein E2-C/UbcH10 blocks cells in metaphase. Proc Natl Acad Sci USA 94: 2362–2367, 1997
56. Percy MJ, Myrie KA, Neeley CK, Azim JN, Ethier SP, Petty EM: Expression and mutational analyses of the human MAD2L1 gene in breast cancer cells [in process citation]. Gen Chrom Cancer 29: 356–362, 2000
57. Gutkind JS: Regulation of mitogen-activated protein kinase signaling networks by G protein-coupled receptors. Science's STKE 1–13, 2000 (*http://www.stke.org/cgi/content/full/OC_sigtrans;2000/40/re1)*
58. Turner CE: Paxillin and focal adhesion signalling. Nat Cell Biol 2: E231–E236, 2000
59. Felsenfeld DP, Schwartzberg PL, Venegas A, Tse R, Sheetz MP: Selective regulation of integrin–cytoskeleton interactions by the tyrosine kinase Src. Nat Cell Biol 1: 200–206, 1999
60. Sieg DJ, Hauck CR, Ilic D, Klingbeil CK, Schaefer E, Damsky CH, Schlaepfer DD: FAK integrates growth-factor and integrin signals to promote cell migration. Nat Cell Biol 2: 249–256, 2000
61. Cavenee WK, Furnari FB, Nagane M, Huang H-JS, Newcomb EW, Bigner DD, Weller M, Berens ME, Plate KH, Israel MA, Noble MD, Kleihues P: Diffusely infiltrating astrocytomas. In: Kleihues P, Cavenee WK (eds) Pathology and Genetics of Tumours of the nervous System. IARC Press, Lyon, 2000, pp 10–21

Address for offprints: Michael E. Berens, Neurology Research, NRC Building, 4th Floor, 350 W. Thomas Rd., Phoenix, AZ 85013, USA; Tel.: 602 406 6664; Fax: 602 406 7172; E-mail:mberens@chw.edu